

Pyrithione-based ruthenium complexes as inhibitors of aldo-keto reductase 1C enzymes and anticancer agents

Jakob Kljun¹, Maja Anko², Katja Traven¹, Maša Sinreih², Renata Pavlič², Špela Peršič¹, Žiga Ude¹, Elisa Esteve Codina^{1,3}, Jure Stojan², Tea Lanišnik Rižner^{2,*}, Iztok Turel^{1,*}

¹ Department for Chemistry and Biochemistry, Faculty of Chemistry and Chemical Technology, University of Ljubljana, Večna pot 113, SI-1000 Ljubljana, Slovenia

² Institute of Biochemistry, Faculty of Medicine, University of Ljubljana, Vrazov trg 2, SI-1000 Ljubljana, Slovenia

³ Faculty of Chemistry, University of Valencia, carrer Doctor Moliner, 50. 46100, Burjassot, Spain

*Corresponding authors:

Dr. Tea Lanišnik Rižner

Institutional address: Institute of Biochemistry, Faculty of Medicine, University of Ljubljana, Vrazov trg 2, SI-1000 Ljubljana, Slovenia

Tel: +386-1-54-37-657; Fax: +386-1-54-37-641; E-mail: tea.lanisnik-rizner@mf.uni-lj.si

Dr. Iztok Turel

Institutional address: Faculty of Chemistry and Chemical Technology, University of Ljubljana, Večna pot 113, SI-1000 Ljubljana, Slovenia

Tel: +386-1-24-19-124; Fax: +386-1-24-19-220; E-mail: iztok.turel@fkkt.uni-lj.si

X-ray crystallography

The structures were solved by direct methods implemented in SIR92¹ and refined by a full-matrix least-squares procedure based on F² using SHELXL-97.² All non-hydrogen atoms were refined anisotropically. The hydrogen atoms were placed at calculated positions and treated using appropriate riding models. The programs Mercury, ORTEP and Platon were used for data analysis and figure preparation.³

Table S1: Crystallographic data for compounds **1A**, **1B**, **2A**, and **2B**.

Compound	1A	1B	(2·2A)·CHCl ₃	2B
Empirical formula	C ₁₅ H ₁₈ ClNO ₂ Ru	C ₁₅ H ₁₈ ClNORuS	C ₂₇ H ₄₅ Cl ₃ F ₁₂ N ₂ O ₆ P ₂ Ru ₂ S ₈	C ₁₃ H ₂₂ F ₆ NO ₂ PRuS ₅
M _w	380.82	396.88	1348.56	630.65
T, K	150(2)	150(2)	150(2)	150(2)
Crystal system	<i>monoclinic</i>	<i>triclinic</i>	<i>orthorhombic</i>	<i>triclinic</i>
Space group	<i>P 21/n</i>	<i>P -1</i>	<i>P nma</i>	<i>P -1</i>
a, Å	6.3748(1)	8.2322(3)	28.7623(4)	7.8145(3)
b, Å	15.2882(3)	8.5818(3)	21.1882(3)	12.1293(5)
c, Å	15.5899(3)	12.0070(4)	7.7865(1)	12.2989(5)
α, deg.	90	73.950(3)	90	99.963(4)
β, deg.	91.866(2)	73.345(3)	90	101.149(4)
γ, deg.	90	89.785(3)	90	107.554(4)
V, Å ³	1518.57(5)	778.37(5)	4745.26(11)	1056.61(8)
Z	4	2	4	2
D _{calc} , g/cm ³	1.666	1.693	1.888	1.982
μ, mm ⁻¹	1.208	1.307	1.313	1.375
F(000)	768	400	2686	632
Crystal size, mm	0.60×0.15×0.15	0.02×0.01×0.01	0.30×0.07×0.07	0.20×0.10×0.02
Color	yellow	yellow	yellow	yellow
Data collected / unique	16431 / 3490	12463 / 3561	47625 / 5583	10394 / 4832
R _{int}	0.0441	0.0386	0.0378	0.0294
Restraints / parameters	0 / 184	0 / 184	0 / 297	0 / 264
S	1.063	1.027	0.679	1.059
R ₁ , wR ₂ [I>2σ(I)]	0.0244 / 0.0576	0.0304 / 0.0641	0.0238 / 0.0608	0.0280 / 0.0525
R ₁ , wR ₂ (all data)	0.0311 / 0.0616	0.0380 / 0.0676	0.0310 / 0.0662	0.0395 / 0.0581
Larg. diff. peak/hole (e ⁻ ·Å ⁻³)	0.475 / -0.465	0.701 / -0.580	0.545 / -0.449	0.452 / -0.408

AKR1C1-C3 inhibition – experimental data

Figure S1: Progress curves for the AKR1C1 catalyzed oxidation of 1-acenaphthenol in the presence of four Ru complexes (1A, 1B, 2A, 2B) and two ligands (LA, LB). The upper curve in each panel is a control without the inhibitor. The concentrations of the inhibitors were 20 μM and 0.1 mM (1A, 2A, 2B, LB), 50 μM and 0.1 mM (LB) and 5 μM and 10 μM (1B). The coenzyme NAD^+ was 2.3 mM and substrate 1-acenaphthenol was 90 μM .

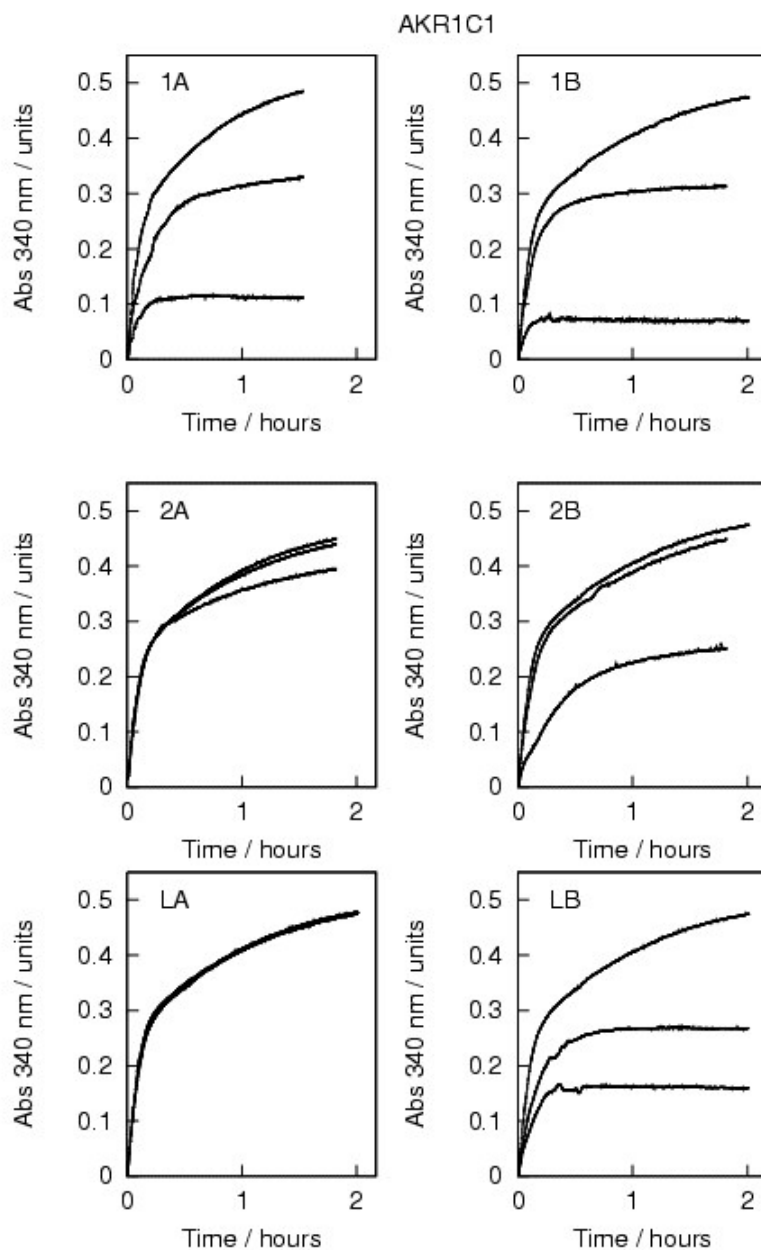


Figure S2: Progress curves for the AKR1C2 catalyzed oxidation of 1-acenaphthenol in the presence of four Ru complexes (1A, 1B, 2A, 2B) and two ligands (LA, LB). The upper curve in each panel is a control without the inhibitor. The concentrations of the inhibitor were 20 μM and 0.1 mM, except for LB with 50 μM and 0.1 mM concentrations. The coenzyme NAD^+ was 2.3 mM and substrate 1-acenaphthenol was 180 μM .

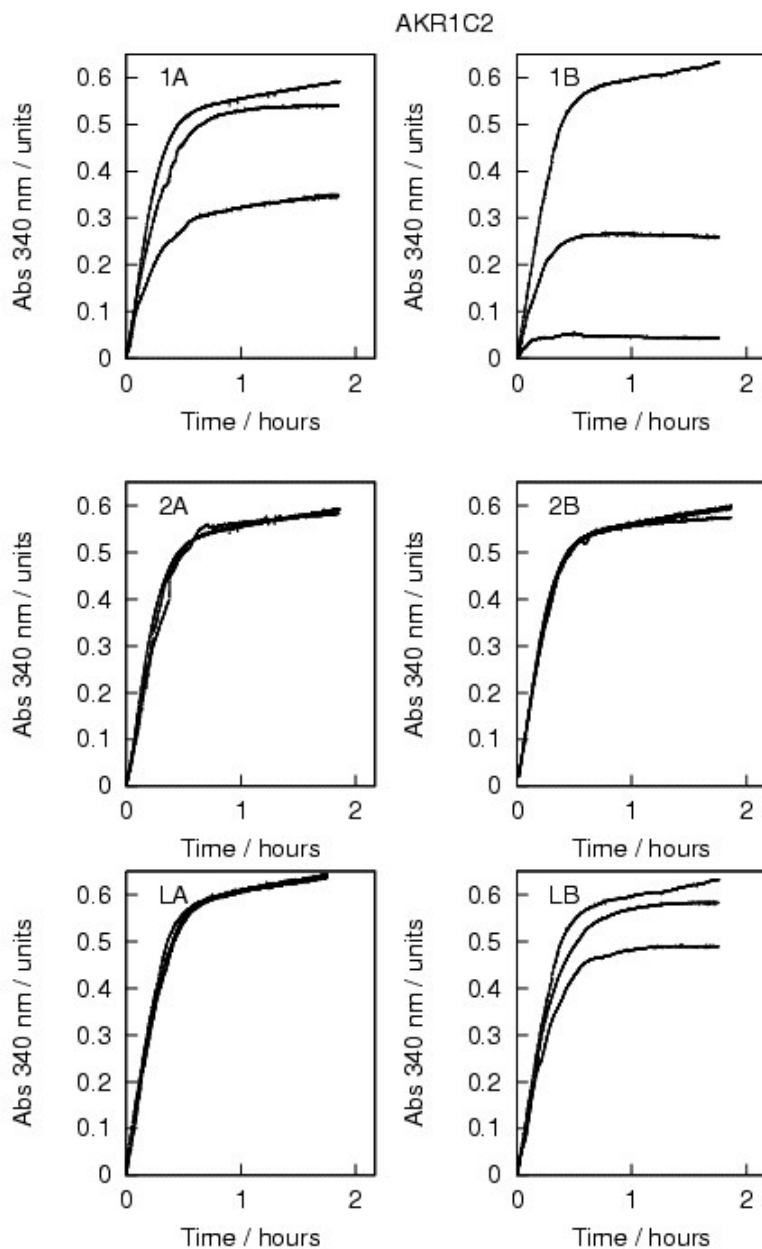


Figure S3: Progress curves for the AKR1C3 catalyzed oxidation of 1-acenaphthenol in the presence of four Ru complexes (1A, 1B, 2A, 2B) and two ligands (LA, LB). The upper curve in each panel is a control without the inhibitor. The concentrations of the inhibitor were 20 μM and 0.1 mM, except for **1B** with 10 μM and 0.1 mM concentrations and **LB** with 35 μM and 0.1 mM concentrations. The coenzyme NAD^+ was 2.3 mM and substrate 1-acenaphthenol was 250 μM .

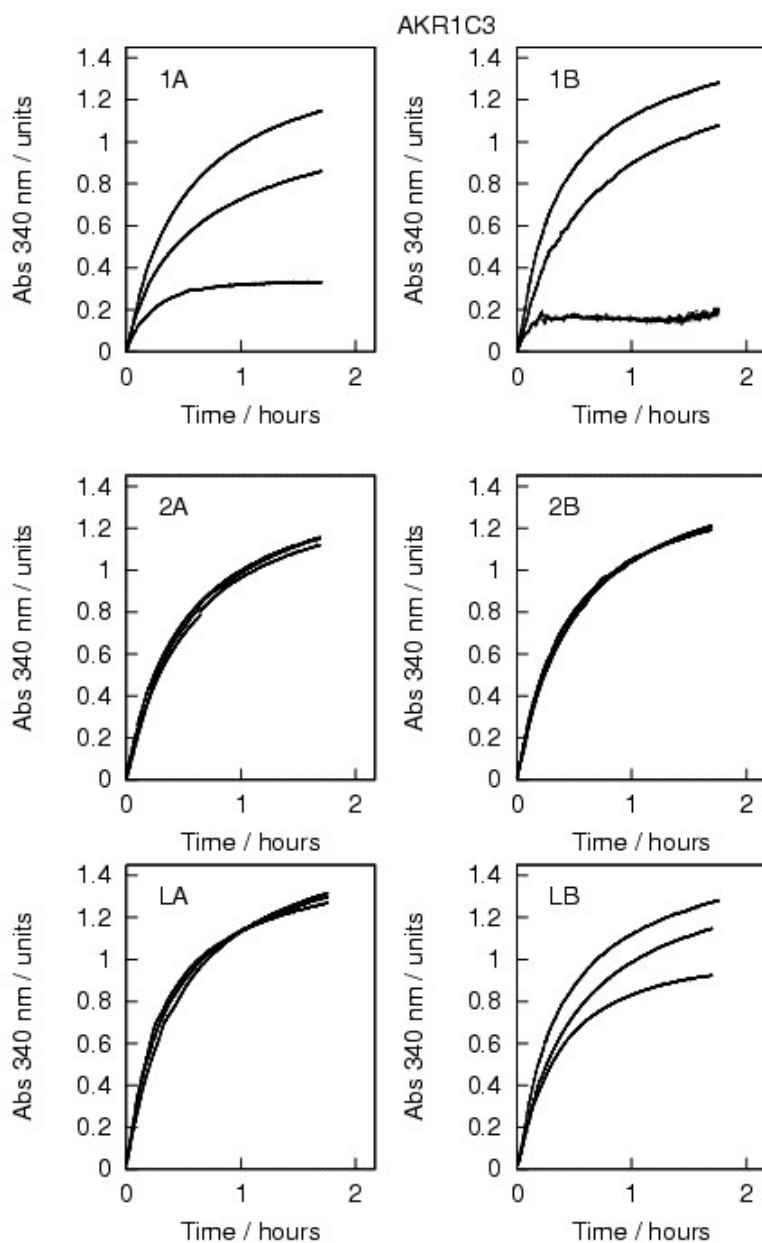
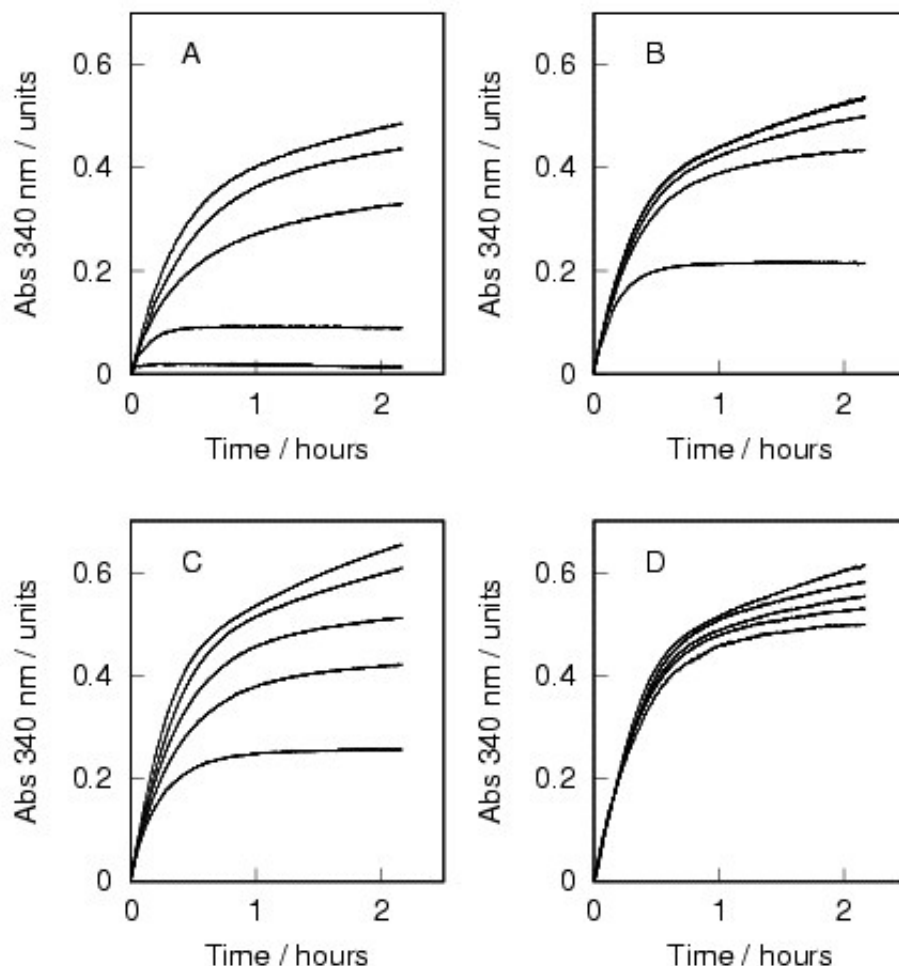
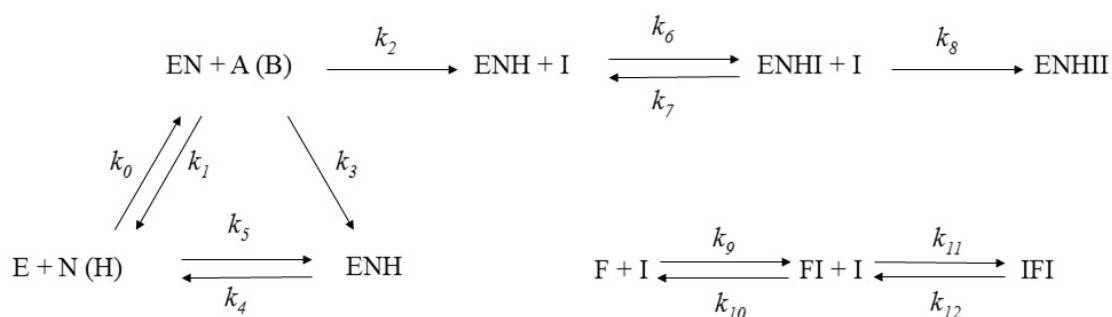


Figure S4: Progress curves for the AKR1C1 catalyzed oxidation of 1-acenaphthenol in the presence of compound 1B without albumin (A) and with addition of 15 μM albumin (B), 75 μM albumin (C) and 150 μM albumin (D). The upper curve in each panel is a control without the inhibitor. The concentrations of 1B were 1.5, 3, 6 and 15 μM (A); 2, 5, 10 and 20 μM (B); 30, 60, 80 and 100 μM (C). The coenzyme NAD^+ was 2.3 mM and substrate 1-acenaphthenol was 0.1 mM.



Scheme S1: Universal scheme for inhibition/inactivation of AKR1C enzymes by Ru complexes and ligands in the presence of albumin. E is free enzyme, N is coenzyme NAD^+ , EN and ENH are enzyme-coenzyme complexes with oxidized and reduced form of coenzyme, respectively, A, B are the enantiomers of 1-acenaphthenol, I is inhibitor, and F is albumin; $k_0 - k_{12}$ are first and second order rate constants.



Stability and reactivity in aqueous media

Figure S5: ^1H NMR spectra of **1B** in 10% $\text{dms}\text{-d}_6$ / D_2O . Bottom – $t = 0$; middle – $t = 20$ min; top – $t = 20$ h.

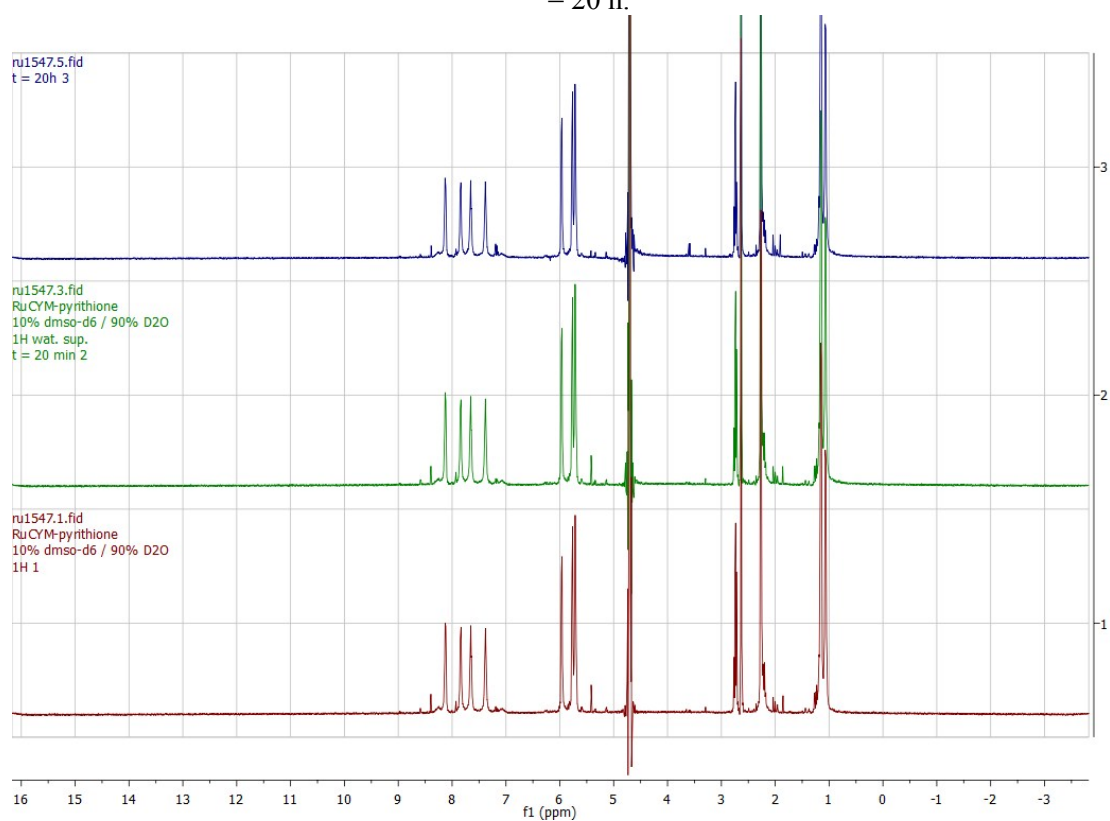


Figure S6: ^1H NMR spectra of His/**1B** reaction mixture in 10% $\text{dms}\text{-d}_6$ / D_2O . From bottom to top: 2A; His; reaction mixture at $t = 0$; $t = 25$ min; $t = 20$ h.

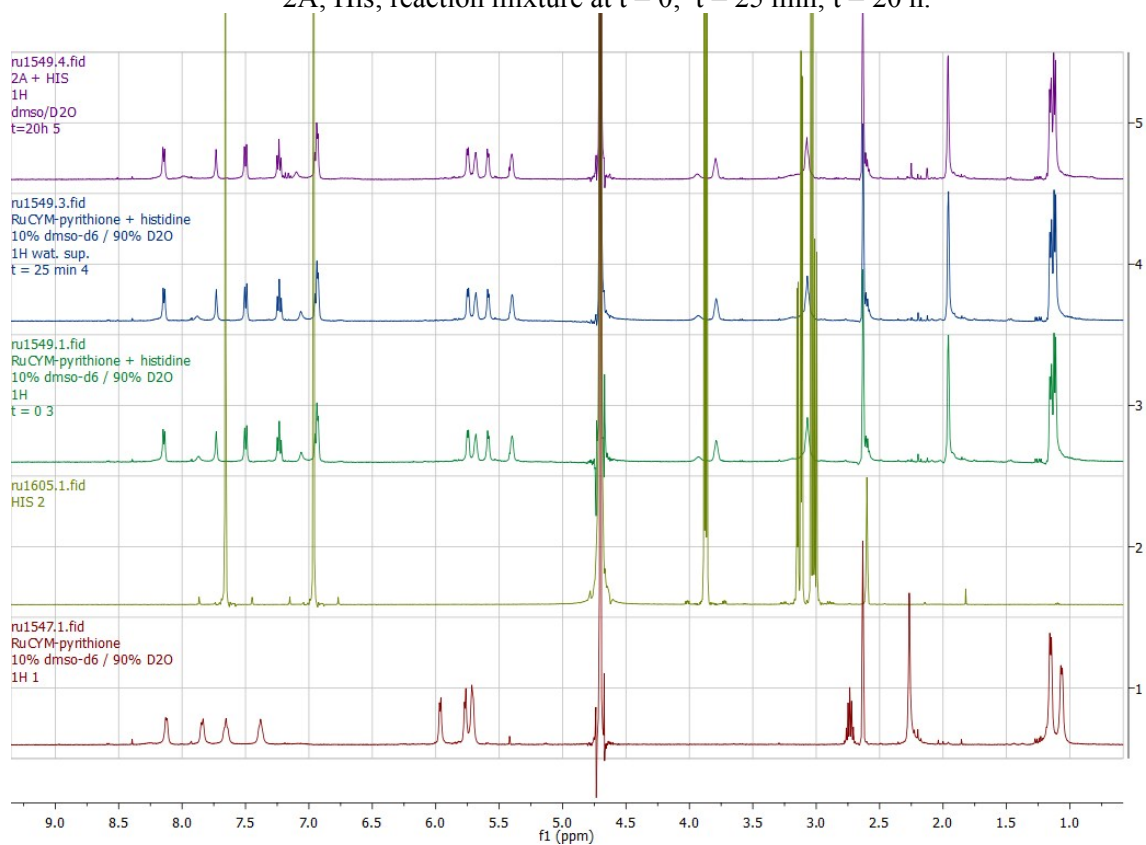


Figure S7: ^1H NMR spectra of Cys/**1B** reaction mixture in 10% $\text{dms}\text{-d}_6$ / D_2O . From bottom to top: 2A; His; reaction mixture at $t = 0$; $t = 25$ min; $t = 20$ h.

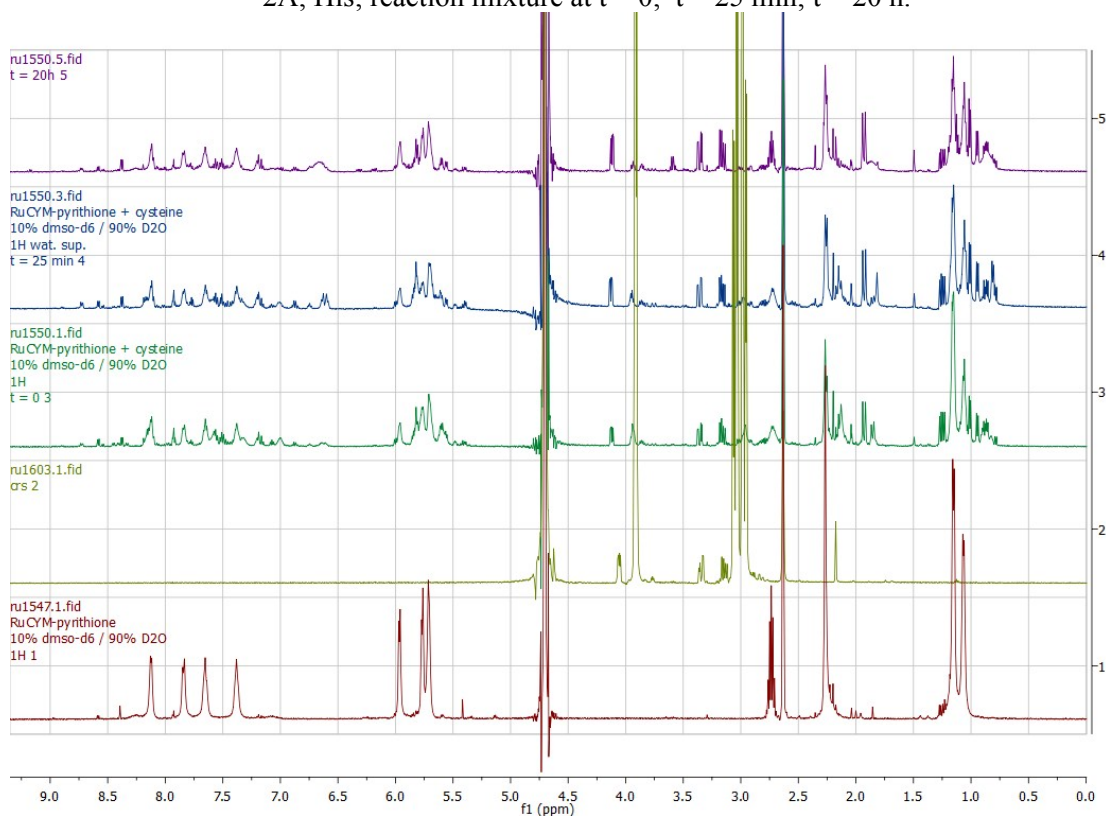


Figure S8: ^1H NMR spectra of Gsh/**1B** reaction mixture in 10% $\text{dms}\text{-d}_6$ / D_2O . From bottom to top: 2A; His; reaction mixture at $t = 0$; $t = 25$ min; $t = 20$ h.

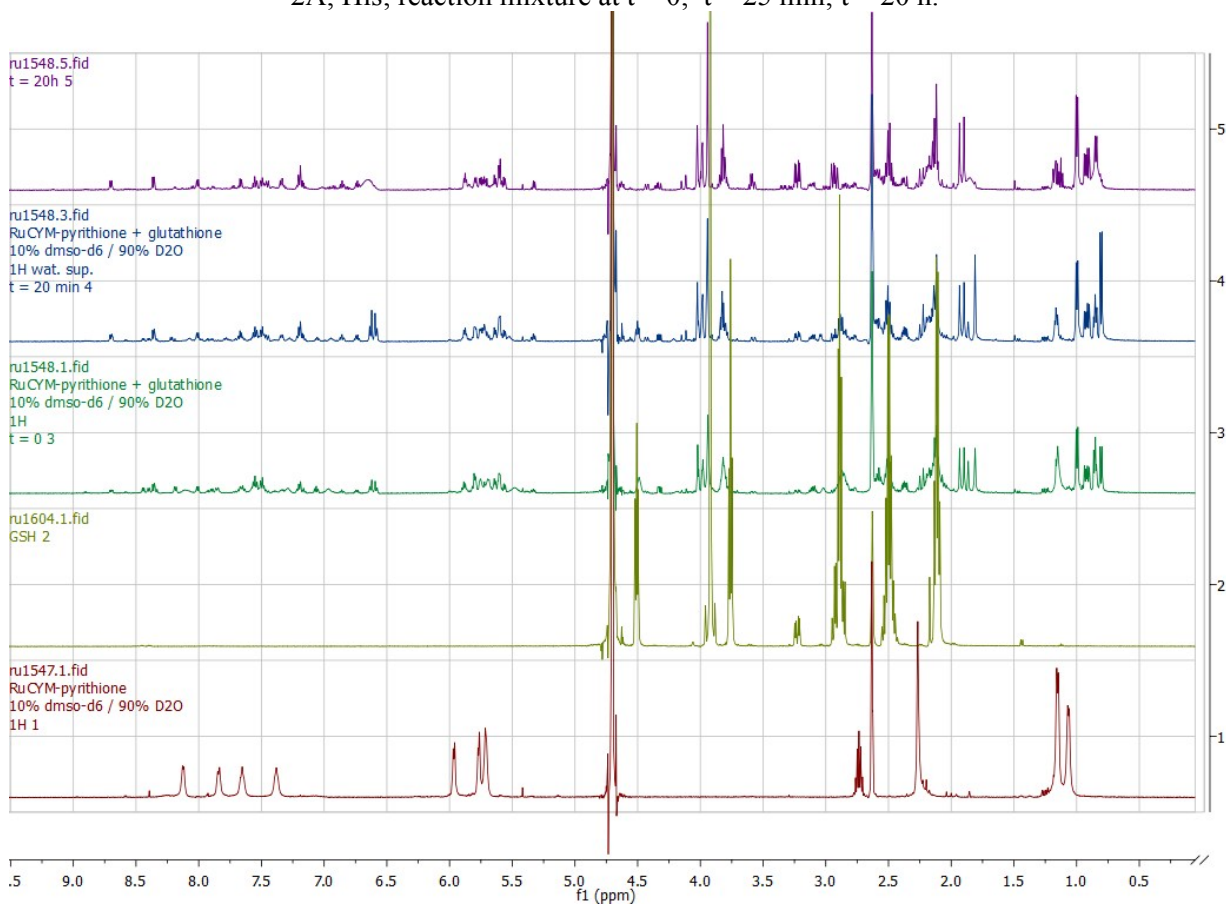
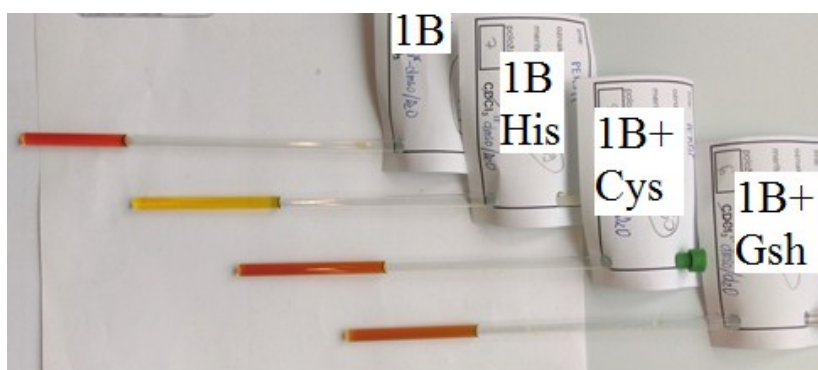


Figure S9: NMR tubes with 1B solutions and reaction mixtures with His, Cys and Gsh.



Cell proliferation assay

The influence of ruthenium compounds on cell proliferation was analyzed using the breast cancer cell line MCF-7 and the cell proliferation reagent WST-1 (Roche Diagnostics, Germany) following the manufacturer's instructions. Cells were cultivated in EMEM medium supplemented with 10% fetal bovine serum, 2 mM glutamine, insulin at 0.01 mg/mL and antibiotics (100 U/L penicillin and 0.1 mg/L streptomycin, all reagents Sigma-Aldrich, Germany). Cells were grown in a humidified atmosphere of 5% CO₂ at 37 °C. Cells in the 13th to 23rd passage were used.

1 · 10⁴ cells were seeded in a 96-well plate in 90 µL of medium and allowed to adhere and grow for 24 h. Ruthenium complexes were dissolved in DMSO as a 2 mM stock solution. Working solutions were prepared by serial dilution of the stock solution with culture medium. After the initial incubation cells were treated with increasing concentrations of ruthenium compounds. Since DMSO affects cultured cells, its concentration was kept below 0.5%. After 48 h incubation period, plates were treated with 10 µL of WST-1 for 4 h. Absorbance was measured with an Epoch microplate spectrophotometer at 450 nm with the reference wavelength set at 600 nm.

All the experiments were performed in triplicates. First, the background value from a well containing active compound without cells was subtracted then average values for the triplicates were calculated. Absorbance of the well containing only non-treated cells was used as a normalization control. The half-maximal effective concentration (EC₅₀) was determined by constructing a dose-response curve (Graph Pad Prism, Version 5.0).

References:

1. Altomare, A.; Cascarano, G.; Giacovazzo, C.; Guagliardi, A. C.; Burla, M. C.; Polidori, G.; Camalli, M., *SIR92 – a program for automatic solution of crystal structures by direct methods. J. Appl. Cryst.* **1994**, *27*, 435.
2. Sheldrick, G. M., A short history of SHELX. *Acta Crystallogr., Sect. A* **2008**, *64*, 112-122.
3. Spek, A. L., Structure validation in chemical crystallography. *Acta Crystallogr., Sect. D: Biol. Crystallogr.* **2009**, *65*, 148-155; Macrae, C. F.; Edgington, P. R.; McCabe, P.; Pidcock, E.; Shields, G. P.; Taylor, R.; Towler, M.; van De Streek, J., Mercury: visualization and analysis of crystal structures. *J. Appl. Cryst.* **2006**, *39*, 453-457.